Theor Chem Acc (1999) 101:114–120
DOI 10.1007/s002149800m76

Theoretical
Chemistry Accounts

Regular article

Sequence dependence of DNA radioprotection by the thiols WR-1065 and WR-151326*

D. Sy[1,2], C. Durand[1], S. Hugot[1], C. Savoye[1], C. Swenberg[3], M. Charlier[1], M. Spotheim-Maurizot[1]

[1] Centre de Biophysique Moléculaire, CNRS, rue Charles-Sadron, F-45071 Orléans Cedex 2, France
[2] Faculté des Sciences, B.P. 6759, Université d' Orléans, F-45067 Orléans Cedex 2, France
[3] Applied Cellular Radiation Biology Department, Armed Forces Radiobiology Research Institute, Bethesda, MD 20889, USA

Received: 24 April 1998 / Accepted: 4 August 1998 / Published online: 11 November 1998

Abstract. Sequence-dependent variations of DNA structure modulate radiation-induced strand breakage. Thiols reduce breakage by scavenging damaging radiolytic $OH^{\cdot}$ and repairing sugar radicals. As shown by sequencing gel electrophoresis, WR-1065 radioprotection is modulated by sequence, whereas that of WR-151326, a larger thiol, is more evenly distributed. Molecular modelling was performed on complexes of a 53 bp oligonucleotide (belonging to a natural restriction fragment) with one molecule of WR-1065 or WR-151326. Energy minimised structures exhibit a broadening of the minor groove of an AAATT motif upon WR-1065 binding, and a narrowing of the groove upon WR-151326 binding. Consequently, the accessibility to $OH^{\cdot}$ of H4′ (whose abstraction leads to strand breakage) increases near WR-1065, whereas it decreases near WR-151326. This modifies locally the otherwise homogeneous radioprotection. The effect of WR-151326 strengthens the protection at all tested binding sites, whereas that of WR-1065 diminishes it in some regions, in good agreement with the observed radioprotection distribution.

Key words: DNA sequence – DNA structure – Molecular modelling – Radioprotection – WR thiols

1 Introduction

The radiation-induced DNA frank strand breakage in anoxic conditions is mainly due to the abstraction of the H4′ atom by the $OH^{\cdot}$ radicals produced by water radiolysis and to the subsequent formation of sugar radicals [1, 2]. The probability of breakage at each nucleotide depends on the sequence via the local structure. For instance, some regions present minor grooves that are narrower, and others broader, than that of the canonical B-DNA. The sequence dependence of radiosensitivity can be explained by the variation of the accessibility to the $OH^{\cdot}$ radicals of the H4′ atoms deeply embedded in the minor groove. Molecular modelling has shown that the accessibility strongly depends on the width of the minor groove. The accessibility of H4′ is a maximum for all regions with a minor groove width (as defined in Ref. [3]) larger than about 4.5 Å and decreases linearly for narrower grooves [4]. Therefore, a minor groove broadening or narrowing induced by the binding of a ligand may increase or decrease radiosensitivity.

Scavenging of $OH^{\cdot}$ radicals and chemical repair of the radiation-induced C4′-centred radicals by donation of a H atom from the SH group are the main mechanisms of DNA radioprotection by thiols [5, 6]. Since they bind strongly to DNA, the positively charged thiols are the best known radioprotectors [7, 8].

The thiol WR-1065 [NH_3-$(CH_2)_3$-NH_2-$(CH_2)_2$-SH] is the main metabolite of the clinically used cytoprotective phosphorothioate WR-2721 (Ethyol, Amifostine) [9]. This thiol bears at 0°C and at neutral pH an electrical charge $Z = +2$ on its amino groups [10] and efficiently protects DNA [8, 11, 12]. Based on molecular modelling with a 30 bp DNA, the variation of protection along the DNA sequence was explained by the conformational changes induced by the binding of the thiol in the minor groove, energetically the most favourable location. This was shown to be, in AT-rich regions, also the preferential binding site of putrescine, a natural diamine with $Z = +2$, at low binding density [13]. Such structural changes lead to broadening or narrowing of the minor grooves of regions with initially (in absence of the thiol) narrow minor grooves [12]. The resulting modifications of accessibility of H4′ can interfere with protection by scavenging and by chemical repair, and explain the higher or lower radioprotection of these regions as compared to a random sequence.

The phosphorothioate WR-151327 is an efficient radioprotector [14, 15] with a lower oral toxicity than WR-2721 [16]. The thiol WR-151326 [CH_3-NH_2-$(CH_2)_3$-

*Contribution to the Proceedings of Computational Chemistry and the Living World, April 20–24, 1998, Chambery, France

Correspondence to: D. Sy

NH_2-$(CH_2)_3$-SH] is its main metabolite. Controversial results on the radioprotective ability of WR-151326 as compared to WR-1065 (higher, equal or lower) are reported [17, 18]. The difference between this thiol and WR-1065 are (1) a longer distance between the central charged amino groups and the SH group, and (2) the association of a methyl group with the terminal amino group, which confers a better uptake of WR-151326 by the tissues [16].

The protections of DNA against fast neutron-induced strand breakage by WR-151326 and WR-1065 were here compared using sequencing gel electrophoresis. Molecular modelling calculations were carried out on a 53 bp DNA for explaining the different sequence dependences of radioprotection for the two thiols.

2 Materials and methods

2.1 Electrophoresis of irradiated DNA-thiol complexes

The DNA fragment of 80 base pairs labelled at the 5′-end of one strand was prepared from the pOP203 plasmid as previously described [19]. It was irradiated at a concentration of 5 μg/ml (1.4×10^{-5} M nucleotide) at 0°C in 1 mM potassium phosphate buffer, pH 7.2. Solutions of WR-151326 and WR-1065 (Walter Reed Army Institute, Washington, D.C.) were prepared in the same buffer. Drugs and DNA solutions were separately deoxygenated by flushing with pure argon, mixed and kept under argon flushing until irradiation to avoid thiol oxidation.

Irradiations were performed with fast neutrons obtained by the nuclear reaction of 34 MeV protons on a semi-thick beryllium target (Centre d'Etudes et de Recherches par Irradiation, CNRS, Orléans). The dose mean lineal energy in water at the point of interest was 87.7 KeV/μm. The mean dose rate was 10 Gy/min.

The sequencing gel electrophoresis of the irradiated fragments was performed as previously described [19]. To identify the bands, Maxam-Gilbert sequencing of purines and of pyrimidines of the same fragment were performed on the same gel. The fixed and dried gels were exposed onto PhosphorImager, which allows scanning and quantitative analysis using the ImageQuant software (Molecular Dynamics).

2.2 Molecular modelling

A 53 bp region of the 80 bp fragment was built up in the standard B-form with the SYBYL 6.3 software (1996, Tripos, St. Louis, Mo.). The thiols were built separately and their positively charged amino groups were anchored on the negatively charged phosphates of four nucleotides (two consecutive nucleotides on each strand). They were placed in the minor groove, parallel to the strands of DNA. For each binding site, the thiol was placed before minimisation at three different distances from the axis of DNA. The energy calculations were performed with the AMBER force field using Kollman's charges with a cut-off distance of 10 Å [20]. The solvent effect was implicitly taken into account by introducing a distance (r) dependent dielectric constant ($\varepsilon = 4r$). The structure of DNA-WR 151326 and DNA-WR-1065 were energy-minimised via the Powell method [21]. The energy of interaction between the ligand and DNA is defined as the difference between the energy of the complex and the sum of the energies of the two partners.

The accessibility of H4′ was calculated with the SAVOL algorithm included in SYBYL. The accessible surface is determined by rolling a sphere of 1.2 Å radius, simulating an $OH^{\cdot}$, on the van der Waals surface of the H-atoms. The minor groove width was measured at each nucleotide site as the mean distance between the centre of the H5′2 atom and the centre of the H4′ atom of the opposite nucleotide [3]. The most appropriate torsional conformation of the thiols in the complexes was obtained after a search in which the last two bonds of the thiol were rotated by steps of 10°. This search was followed by a new energy minimisation of the complex structure.

3 Results

3.1 Radiolysis of the 80-bp restriction fragment

Deoxygenated solutions of ^{32}P-labelled 80-bp restriction fragments were irradiated at 0°C with 80 Gy of fast neutrons in the absence or in the presence of WR-1065 or WR-151326. The probability of breakage at each nucleotide site was determined from the sequencing gel electrophoresis patterns. For the naked (without ligand) DNA, the probability is lower in several regions along the fragment, as previously reported [4]. Variations of breakage probabilities are also observed for the samples irradiated in the presence of the thiols. At identical concentrations (0.07 WR/nucleotide), the protection pattern (pattern of ratios of the breakage probability at each nucleotide of the DNA with and without ligand) of WR-151326 is almost homogeneous, whereas that of WR-1065 is strongly sequence-modulated. A comparison of the two protection patterns (averages of four independent experiments) is presented in Fig. 1. The nucleotides of region A (G6T19) are slightly less protected by WR-151326 than by WR-1065. The nucleotides of the region B (G20G33), well protected

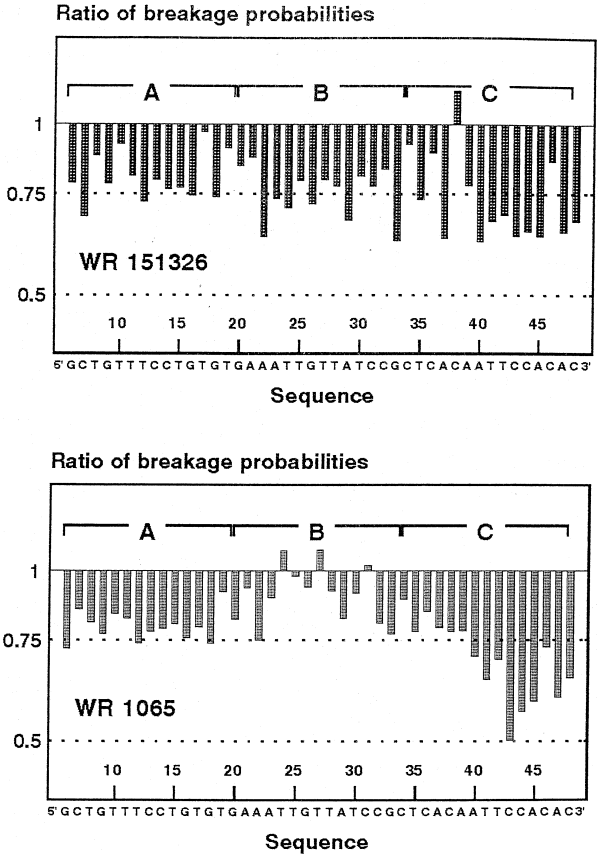

Fig. 1. Ratios of the probability of strand breakage at each nucleotide site of the 80 bp fragment irradiated in deoxygenated solution in the presence ($R = 0.07$) and in the absence of WR-151326 or WR-1065. Irradiation dose: 80 Gy of fast neutrons

by WR-151326, are much less protected by WR-1065. The nucleotides of region C (C34T47) are slightly better protected by WR-1065 than by WR-151326. Globally, the fragment is equally protected by the two thiols, with PF $\approx$ 1.3 (average value over all nucleotides).

3.2 Molecular modelling

On the energy-minimised 53 bp structure, the minor groove width and the accessibility of H4′ atoms to an $OH^{\cdot}$ radical were calculated. The variations along the sequence of the minor groove width and of the H4′ accessibility previously reported for a 68 bp naked DNA [4] are again observed. The H4′ accessibility is strongly decreased for minor grooves narrower than the critical value 4.5 Å (Figs. 2, 3).

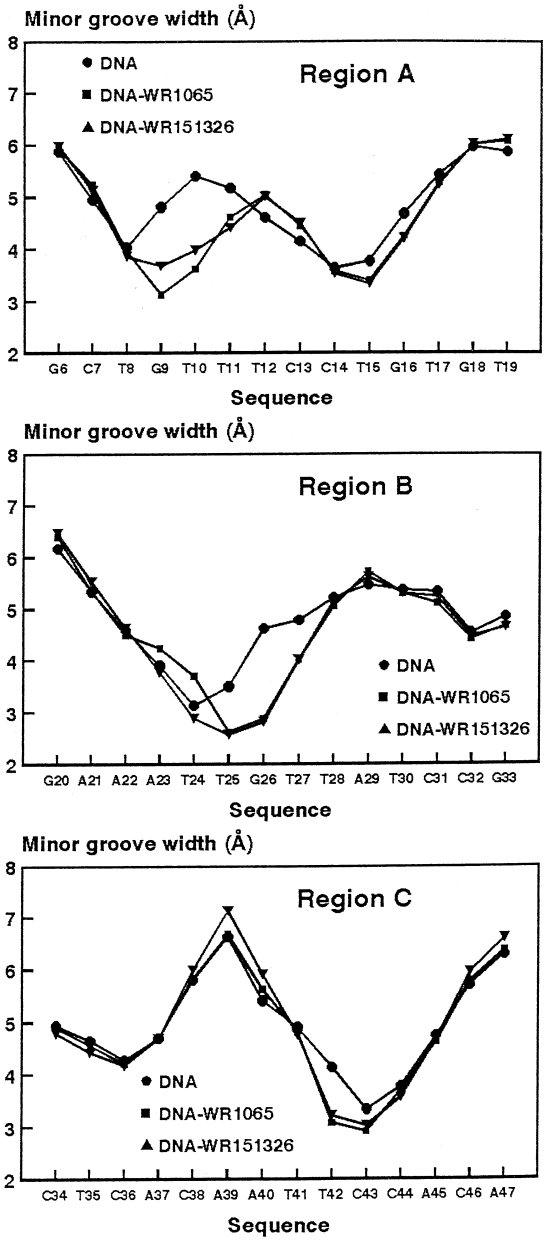

Fig. 2. Minor groove width along parts of the 53 bp model DNA, without or with thiols bound to: T10T11 (*region A*), G26T27 (*region B*) and C43C44 (*region C*)

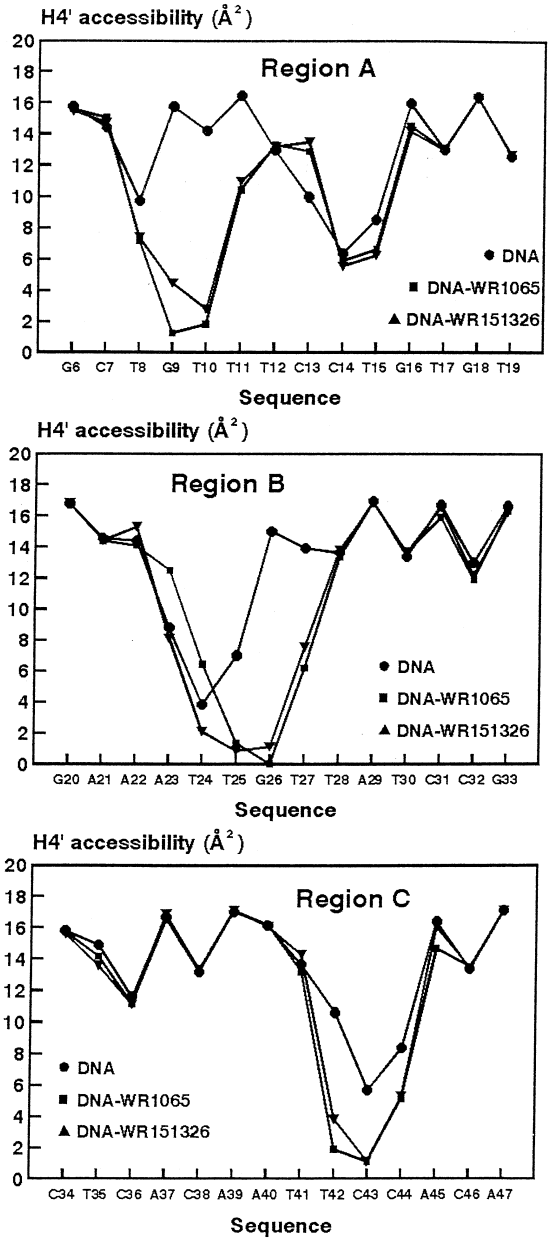

Fig. 3. Accessibility of H4′ atoms to $OH^{\cdot}$ radicals along parts of the 53 bp model DNA, without or with thiols bound to: T10T11 (*region A*), G26T27 (*region B*) and C43C44 (*region C*)

The thiols were positioned parallel to the strands in the minor groove of DNA, the energetically most favourable binding location [12]. The preference for the binding in the minor groove is due to the global shape and linear conformation of the thiol, to the low electrostatic potential of the groove and to the good match of the distance between two positively charged amino groups and the distance between the two negatively charged phosphate groups of two consecutive nucleotides of a strand.

The amino groups of the thiols were initially anchored on the phosphate groups of four nucleotides (two

nucleotides on each strand) of the 53 bp (106 nucleotides) DNA. Several sites along the sequence (at least three sites in each region: A, B and C) were tested. For each site, three distances of the thiol to DNA axis were considered. After energy minimisation, the conformation of DNA, the position of the thiol along the sequence, and the distance with respect to the DNA axis and the thiol conformation changed. Thus, the minor groove width around the binding site (even 3–4 nucleotides away) was either increased or decreased, the thiols having slipped along the sequence and become either closer to or farther away from the DNA.

The complexes with, relatively, the slightly stronger interactions (lowest negative interaction energy) are those with the thiol initially anchored on the strand of interest (labelled in the experiments) to T10T11 (in region A), G26T27 (in region B) or C43C44 (in region C). The width of the minor groove was analysed along these regions (Fig. 2).

The accessibility of H4′ atoms to $OH^{\cdot}$ radicals was calculated by determining the accessible surface of H4′ atom of each nucleotide, to a sphere of the size of an $OH^{\cdot}$ radical (Fig. 3). To observe the influence of the presence of the thiol on the reduction of accessibility (masking effect), the accessibility was also calculated after extracting the thiol. The sites where extraction leads to an increase of accessibility are those which were masked by the thiol.

3.2.1 Region A of the 53 bp DNA with the thiol anchored on T10T11.

In the naked DNA the minor groove is narrower than the critical value 4.5 Å only at T8. The binding of the two thiols at T10T11 extends the zone of the narrow minor groove over three additional nucleotides (G9-T11). The decrease of the minor groove width is slightly less important for WR-151326 than for WR-1065. The accessibility is reduced at T8-T11. The masking effect is observed at G9-T11 for WR-151326 and at T10T11 for WR-1065. The narrowing of the minor groove in the DNA-WR 151326 complex as compared to naked DNA can be observed in Fig. 4.

3.2.2 Region B of the 53 bp DNA with the thiol anchored on G26T27.

In the naked DNA, the minor groove is narrower than 4.5 Å along A22-G26. This is the narrowest groove along the studied fragment. It is also most extended zone with a narrow minor groove (five nucleotides).

In the energy-minimised DNA-WR-151326 complex, the CH_3 extremity of the thiol is shifted towards the exterior of the groove, whereas the shorter WR-1065 is entirely inserted into the very narrow groove (Fig. 5). The binding of the WR-151326 to G26T27 narrows the minor groove from A23 to T27. The binding of WR-1065 widens the initially very narrow groove at A23T24 and then narrows it at T25-T27. The difference in the groove width in the A23T24 region can be observed in Fig. 5. The accessibility is reduced at T24-T27 for WR-151326 and at T25-T27 for WR-1065. It is increased at A23 and T24 for WR-1065. The masking effect is observed at T25G26T27 for WR-151326 and at G26T27 for WR-1065.

3.2.3 Region C of the 53 bp DNA with the thiol anchored on C43C44.

In the naked DNA the minor groove is narrower than 4.5 Å along T42-C44. The binding of WR-151326 or WR-1065 narrows the minor groove at T42-T43 (Fig. 6). The masking effect is observed at T42C43C44 for WR-151326 and at C43C44 for WR-1065.

Thus the calculations of the accessibility of H4′ atoms to $OH^{\cdot}$ radicals exhibit a strong decrease in the regions that present (after the binding of the thiols) a minor groove narrower than 4.5 Å. They are increased in the regions that undergo a widening of an initially narrow groove. The masking effect contributes to the reduction of the accessibility at two or three nucleotides.

The chemical repair process involves the replacement of the H4′ atom (abstracted by the $OH^{\cdot}$ radical) by the H

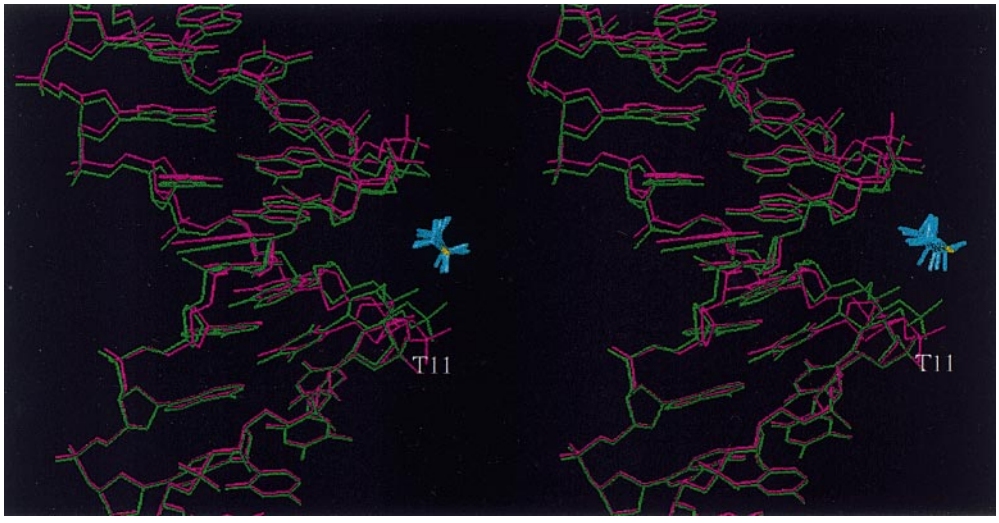

Fig. 4. Stereo-view of the superposition of the energy-minimized structures of the naked DNA and of the DNA-WR-151326 complex with the thiol initially placed around T10T11 (*region A*). Naked DNA is coloured in *magenta*, DNA in the complex in *green* and the thiol in *cyan* (the S atom is *yellow*). One observes the narrowing of the minor groove due to the ''pinching'' of the groove by the thiol

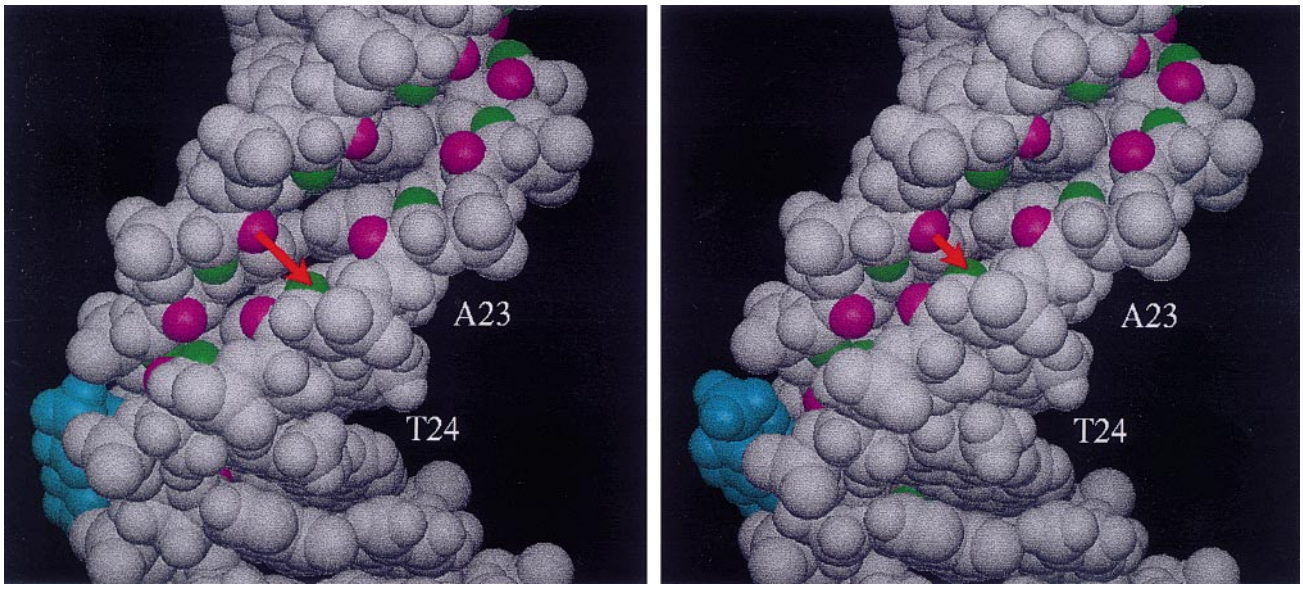

Fig. 5. CPK views of parts of the energy-minimised structures of the region B around A23T24 in the DNA-WR-1065 complex (*left*) and in the DNA-WR-151326 complex (*right*). The thiols initially placed around G26T27 are coloured in *cyan*, the H4′ in *magenta*, the H5′2 in *green*. One observes the different location and insertion of the amino (*left*) or methyl (*right*) groups of the thiols into the minor groove and the different minor groove widths around T24 (*red arrows*)

atom of the SH function. Therefore, we have measured the distances between the H atom of the SH function and the C4′ atom for the six considered complexes. For this purpose, the three terminal bonds of the thiol (C—C, C—C, C—S) were rotated. On the further energy-minimised structure, the energies of interaction and the distances between the H of the thiol functions and the C4′ atom of the closest sugar were measured. The interaction energy was not significantly modified by the rotation. The shortest C4′-H(S) distances are close to 3 Å for all situations.

4 Discussion

Our experimental results show that WR-1065 and WR-151326 globally radioprotect the 80 bp restriction fragment with the same efficiency. The difference between the protection by the two thiols concerns only the sequence dependence of the protection: the protection by WR-1065 is strongly modulated by the sequence, whereas that by WR-151326 is more evenly distributed along the fragment (Fig. 1). The most obvious difference occurs in the regions that are the most radioresistant in the naked DNA (with low accessibility and with minor grooves narrower than 4.5 Å) (Fig. 2).

The results can be discussed in terms of several protection mechanisms. Owing to the presence of the two positive charged amino groups and to the low thiol concentration, all thiol molecules strongly bind to DNA. Therefore they efficiently protect by: (1) scavenging $OH^{\cdot}$ radicals near DNA and thus avoiding H4′ abstraction and consequently strand breakage; (2) chemical repair of the damaged sugars (C4′ centred radicals) by the donation of the H atom of the SH function [the C4′-H(S) distance is compatible with this reaction]. The calculated energies of interaction between the thiol and DNA do not significantly depend on the binding site along the DNA sequence (variations of 5%). Consequently, the thiol binds without a strong sequence preference, and thus one can assume that the two mechanisms contribute to the protection in a sequence-independent manner.

The sequence-dependent variations of protection by WR-1065 were previously qualitatively explained by the modification of the accessibility to $OH^{\cdot}$ radicals of the H4′ atoms, owing to the binding of the thiol. The binding induces structural changes in particular DNA regions (presenting initially a narrow minor groove) such as an additional narrowing or widening of the minor groove [12]. A recent quantitative study on a naked DNA showed that the accessibility of H4′ atoms is maximum for a minor groove width >4.5 Å and decreases linearly with decreasing width below this value [4]. Therefore one can deduce that the modification of the minor groove width influences dramatically the accessibility of H4′ atoms only where the width is initially smaller than 4.5 Å. In the present paper we have quantified the modifications of the minor groove width, and of the accessibility of H4′ atoms induced by the binding of WR-1065 or WR-151326. The results support the already suggested contribution of two additional phenomena on protection by thiols.

4.1 Thiol-induced structural changes around the binding site

Molecular modelling calculations show that the binding of the thiol induces a modification of the minor groove width in regions of 3–5 nucleotides around the binding site. A narrowing of the minor groove is observed around all the tested sites of binding of WR-151326 and a part of those of WR-1065 (Fig. 2). It is due to the

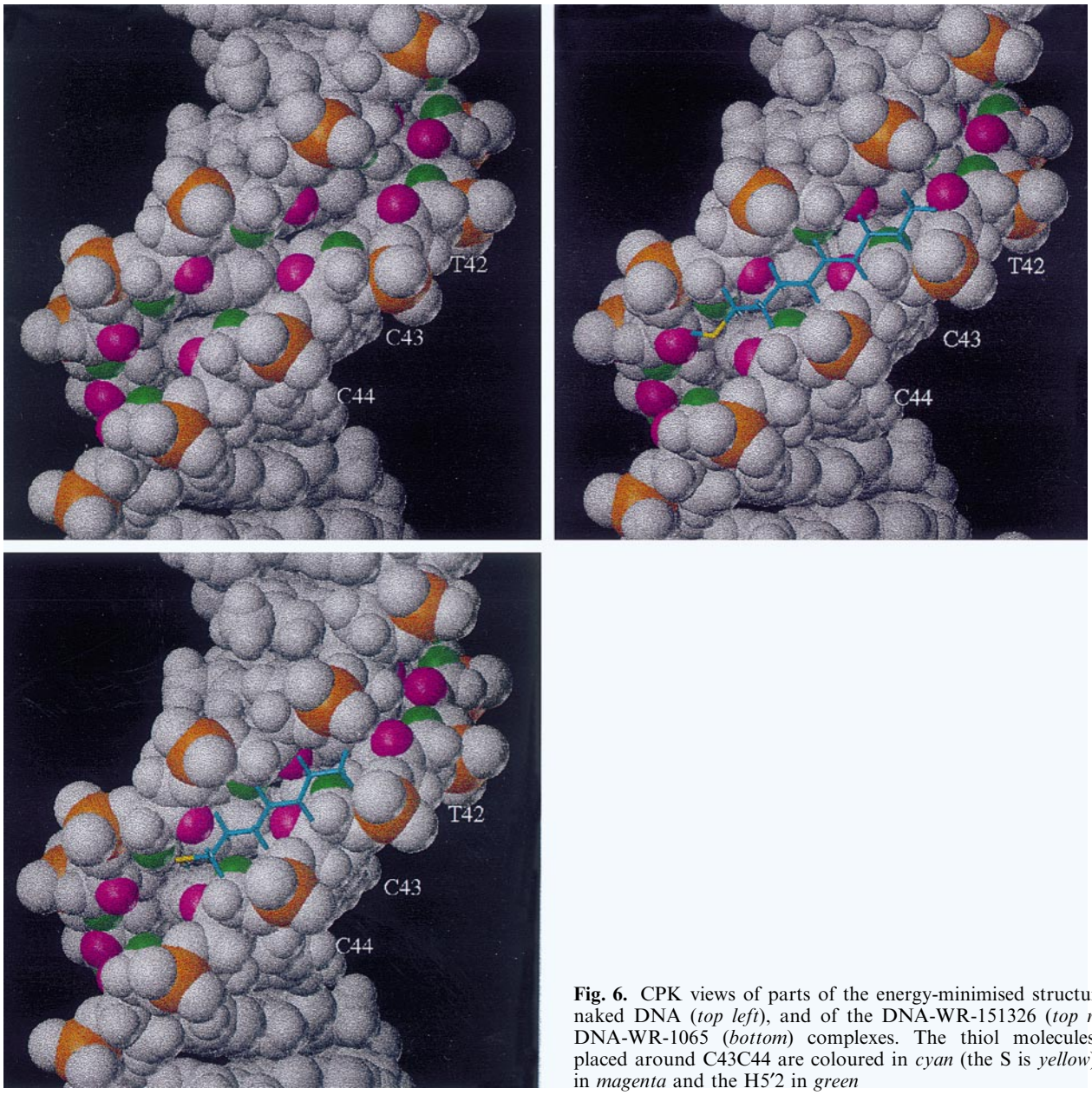

Fig. 6. CPK views of parts of the energy-minimised structures of the naked DNA (*top left*), and of the DNA-WR-151326 (*top right*) and DNA-WR-1065 (*bottom*) complexes. The thiol molecules initially placed around C43C44 are coloured in *cyan* (the S is *yellow*), the H4′ in *magenta* and the H5′2 in *green*

"pinching" of the groove edges by the thiols that are located outside the groove (Fig. 4). The additional narrowing of the groove in regions with an initially (without ligand) narrow minor groove leads to an additional reduction of accessibility of the H4′ atoms (Fig. 3). This phenomenon strengthens the protection in this zone since it gets added to the scavenging the chemical repair afforded by the thiol.

Nevertheless, for the DNA-WR-1065 complex, a slight opening of the groove at two nucleotides located adjacent to the binding site is observed at A23T24 (Fig. 5, left). It belongs to the region with the narrowest minor groove over the entire fragment. It is also the most extended region with a narrow minor groove (five nucleotides). Such a structure can "accept" the deep insertion of the short thiol, but not of the longer one. The steric hindrance of the CH_3 group of WR-151326 (4 Å) is larger than the width of the minor groove just in front of the methyl group (3 Å). The width at this precise site is very narrow because of the strong hindrance due to the two opposite bulky phosphate groups. Therefore the thiol has to adopt a position more exterior to the groove (Fig. 5, right). The opening of the groove owing to the relative insertion of WR-1065 leads to an increase of the accessibility of H4′ atoms. This partially cancels the protection by scavenging and chemical repair in this zone.

4.2 Masking of H4′ atoms by the bound thiol

The protection can be increased also by a decrease of accessibility due to the masking effect. The thiols serve as a shield against the hydroxyl radicals. In all considered complexes, WR-151326 and WR-1065 are masking the

backbone H atoms of respectively three and two nucleotides.

The molecular modelling calculations were performed for a limited number of binding positions – three in each A, B and C regions. Only one of those structures was discussed above. Obviously, for a complete description of the protection pattern, calculations for thiols bound to each nucleotide sites along the fragment (X1X2, X2X3, X3X4 ...) should be performed. Moreover, the thiol should be placed with the SH group pointing also downstream and not only in the upstream 5′-3′ direction of the sequence. Such results should then be added with weights related to the different binding energies. Last, the present molecular modelling calculations were carried out without explicit water molecules and should be extended to systems with water and counterions. However, preliminary calculations on such systems for a shorter sequence show the same effect of ligand-induced minor groove width variations.

5 Conclusion

Although WR-151326 and WR-1065 protect the 80 bp restriction fragment with the same global efficiency (PF = 1.3 for 0.07 thiol/nucleotide), the protection patterns are partially different. The discrepancies between the radioprotection by WR-151326 and WR-1065 in regions with a narrow minor groove can be explained on the basis of molecular modelling calculations. Because of their different sizes the two thiols are differently located with respect to DNA and therefore induce different modifications of the minor groove width. They lead to different modifications of the accessibility of some radiolytic attack sites.

The fact that the entire DNA fragment is almost equally protected by WR-151326 may be an important advantage of this thiol. No region seems to remain unprotected or to become sensitised in the presence of it, as is the case of WR-1065. The suggested advantage of the prodrug WR-151327 over WR-2721 (Ethyol) as a protector of normal tissues during radiotherapy should be checked in detail.

Acknowledgements. We thank Christelle Saint-Marc and Sylvie Gigou for their devoted technical assistance and Roland Sabattier and the staff of Centre d'Etudes et de Recherches par Irradiation, CNRS, Orléans, for the irradiation facilities. This work was partially supported by a grant from Electricité de France (contract RB 96.30).

References

1. Von Sonntag C (1987) Chemical basis of radiation biology. Taylor & Francis, London
2. Giese B, Beyrich-Graf X, Erdmann P, Petretta M, Schwitter U (1995) Chem Biol 2:367
3. Neidle S (1982) FEBS Lett 298:97
4. Sy D, Savoye C, Begusova M, Michalik V, Charlier M, Spotheim-Maurizot M (1997) Int J Radiat Biol 72:147
5. Fahey RC (1988) Pharmacol Ther 39:101
6. Held K (1988) Pharmacol Ther 39:123
7. Spotheim-Maurizot M, Franchet-Beuzit J, Sabattier R, Charlier M (1991) Int J Radiat Biol 59:1313
8. Zheng S, Newton GL, Ward JF, Fahey RC (1992) Radiat Res 130:183
9. Van der Vijght WJF, Peters GJ (1994) Semin Oncol 21 [Suppl 11]:2
10. Newton GL, Dwyer TJ, Kim T, Ward JF, Fahey RC (1992) Radiat Res 131:143
11. Aguilera JA, Newton GL, Fahey RC, Ward JF (1992) Radiat Res 130:194
12. Savoye C, Swenberg C, Hugot S, Sy D, Sabattier R, Charlier M, Spotheim-Maurizot M (1997) Int J Radiat Biol 71:193
13. Lavery R, Sklenar H, Pullman B (1986) J Biol Struct Dyn 3:1015
14. Grdina DJ, Wright BJ, Carness BA (1991) Radiat Res 128:S124
15. Matsushita S, Ando K, Koike S, Grdina DJ, Furukawa S (1994) Int J Radiat Oncol Biol Phys 30:867
16. Green D, Bensely D, Schein P (1994) Cancer Res 54:738
17. Sigdestad CP, Berquist BL, Grdina DJ (1991) Cell Prolif 24:271
18. Balcer-Kubiczek EK, Harrison GH, Hill CK, Blakely WF (1993) Int J Radiat Biol 63:37
19. Franchet-Beuzit J, Spotheim-Maurizot M, Sabattier R, Blazy-Baudras B, Charlier M (1993) Biochemistry 32:2104
20. Weiner SJ, Kollman PA, Case DA, Singh UC, Ghio C, Alagona G, Profeta S Jr, Weiner P (1984) J Am Chem Soc 106:765
21. Powell MD (1977) Math Prog 12:241